Decoherence measurements during the free evolution of a Josephson quantum bit: the quantronium

G. Ithier[1], E. Collin[1], P. Joyez[1], P. Meeson[1], D. Vion[1], and D. Esteve[1]

F. Chiarello[2]

A. Shnirman[3], Y. Makhlin[3], and G. Schön[3]

[1] *Quantronics Group, Service de Physique de l'Etat Condensé, Direction des Sciences de la Matière, CEA-Saclay, 91191 Gif-sur-Yvette, France*

[2] *Istituto di Fotonica e Nanotecnologia, CNR, Via Cineto Romano, 42 00156 Roma, Italy*

[3] *Institut für Theoretische Festkörperphysik, Universität Karlsruhe, 76128 Karlsruhe, Germany*

Abstract: We have measured relaxation and coherence times of a Josephson quantum bit (qubit), the quantronium, during its free evolution, as a function of its biasing point. Several coherence times are obtained from complementary techniques such as resonance linewidth, Ramsey fringes, detuning pulse or spin-echo-like measurements. We explain their variations by a simple model involving modified *1/f* charge and phase noise spectral densities.

Key words: quantum bits, Josephson junctions, quantum coherence.

1. INTRODUCTION

Superconducting circuits based on Josephson junctions can behave quantum mechanically with a coherence time long enough to perform simple manipulations of their quantum state [1-3]. These circuits are potential candidates for implementing quantum bits. Nevertheless, decoherence due to the coupling between the qubit and its environment still severely hinders using these circuits for the development of a quantum processor [4]. The quantitative characterization and understanding of decoherence processes is thus a central issue. In this work, we present experiments that characterize decoherence in a particular Josephson qubit, the quantronium [2], for which atomic physics-like and NMR-like manipulation has been demonstrated [5].

In the next section, we describe the experimental setup and its noise sources, and we give the relevant theoretical decoherence rates. In section 3, we explain how we characterize decoherence at different biasing point and the experimental results are shown and interpreted within a simple model for the noise.

2. THE QUANTRONIUM CIRCUIT AND ITS DECOHERENCE SOURCES

2.1 Principle

The quantronium circuit, schematized on Fig. 1, is derived from the Cooper pair box [6-8]. It consists of a superconducting loop interrupted by two adjacent small Josephson junctions with Josephson energies $E_J(1 \pm d)/2$, with d an asymmetry coefficient made as small as possible, and by a larger Josephson junction ($E_{J0} \approx 15\, E_J$) for readout. The island between the small junctions, with total capacitance C_Σ and charging energy $E_C = (2e)^2/2C_\Sigma$, is biased by a voltage source U through a gate capacitance C_g. The eigenstates of this system are determined by the dimensionless gate charge $N_g = C_g U/2e$, and by the superconducting phase $\delta = \gamma + \varphi$ across the two small junctions, where γ is the phase across the large junction and $\varphi = \phi/\varphi_0$, with ϕ the external flux through the loop and $\varphi_0 = \hbar/2e$. The two lowest energy states $|0\rangle$ and $|1\rangle$ form a qubit, whose transition frequency ν_{01} depends on the bias point $P = (\delta, N_g)$. At the optimal working point $P = (\delta = 0, N_g = 1/2)$, ν_{01} is stationary, which makes the quantronium insensitive to noise at first order [7-8]. For readout [2,8], a trapezoidal readout pulse $I_b(t)$ with a peak value slightly below $I_0 = E_{J0}/\varphi_0$ is applied so that the switching of the large junction to a finite voltage state is induced with a large probability p_1 for state $|1\rangle$ and with a small probability p_0 for state $|0\rangle$. The manipulation of the qubit state is achieved by applying $N_g(t)$ and $I_b(t)$ pulses. When a nearly resonant microwave modulation $\Delta N_g \cos(2\pi\nu_{\mu w} t + \chi)$ is applied to the gate, the Hamiltonian $\hat{h}$ described in a frame rotating at the microwave frequency, is that of a spin 1/2 in an effective magnetic field $\vec{H}$:

$$\hat{h} = -\vec{H}.\vec{\sigma}/2 \quad , \quad \vec{H} = h\Delta\nu\vec{z} + h\nu_{R0}\left[\vec{x}\cos\chi + \vec{y}\sin\chi\right] \qquad (2.1)$$

Here, $\Delta\nu = \nu_{\mu w} - \nu_{01}$ is the detuning, and $\nu_{R0} = 2E_C \Delta N_g \langle 1|\hat{N}|0\rangle/h$ the Rabi frequency. Rabi precession of the spin takes place around an axis with polar angles $\theta = \pi/2 - \arctan(\Delta\nu/\nu_{R0})$ and χ. In the absence of microwave, the spin rotates around Z at the frequency $-\Delta\nu$. Rotations around Z can also

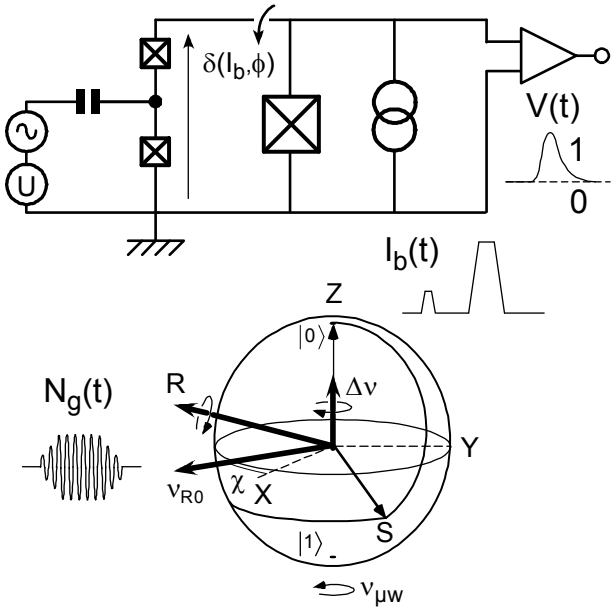

Figure 1. Top: Circuit diagram of the quantronium qubit. The control parameters are $N_g = C_g U / 2e$ *and the phase* δ*, which is determined by the flux* ϕ *imposed through the loop and by the bias-current* I_b*. The qubit state is read out by inducing the switching of the larger readout junction to a finite voltage V with a bias-current pulse* $I_b(t)$*. Bottom: Bloch sphere representation in the rotating frame. Gate microwave pulses induce rotations of the effective spin S around the R axis, whereas adiabatic* $N_g(t)$ *or* $I_b(t)$ *pulses induce rotations around Z.*

be performed by trapezoidal N_g or I_b detuning pulses [5], the rotation angle being in this case proportional to the time integral of $\Delta\nu$.

2.2 Experimental implementation

The sample used for this work was fabricated using standard e-beam lithography and double angle shadow evaporation of aluminum. The readout junction was also connected to a parallel on-chip coplanar gold capacitor of order $C_J \approx 0.6$ pF, in order to lower its plasma frequency. Separate gates with capacitances 40 and 80 aF were used for the DC and microwave N_g signals, respectively. The sample was mounted in a copper shielding box thermally anchored to the mixing chamber of a dilution refrigerator with base temperature 15 mK. The impedance of the microwave gate line as seen from the qubit was defined by a 50 Ω attenuator placed at 600 mK. That of the DC gate line was defined below 100 MHz by a 1 kΩ resistor at 4 K, and its real part was measured to be close to 80 Ω in the 6-17 GHz range explored by the qubit frequency. The bias resistor of the readout junction, R_b=4.1 kΩ, was placed at the lowest temperature. Both the current bias line and the voltage measurement lines were shunted above a few 100 MHz by two surface

mounted 100Ω-47 pF RC shunts. The microwave gate pulses used to manipulate the qubit were generated by mixing continuous microwaves with 1 ns rise time trapezoidal pulses of variable duration τ (defined as the time between 50 % of the rise and 50 % of the fall). The switching probability p was measured over 25000-60000 events with a 10-60 kHz repetition rate. The relevant parameters $E_J = 0.87\ k_BK$, $E_C = 0.66\ k_BK$, $\nu_{01}(P_0) = 16.41$ GHz, d = 3 - 4 %, $I_0 = 427$ nA measured as reported in a previous work [9]. The readout sensitivity was optimized by using 100 ns wide readout pulse ending at $\delta_M \approx 130°$. The fidelity, *i.e.* the largest achieved value of $p_1 - p_0$, was $\eta \approx 0.3$ - 0.4, which is greater than in our previous work [2], but nevertheless much smaller than the 0.95 expected. This loss of visibility is attributed to spurious relaxation of the qubit during the adiabatic ramp used to switch the readout on. Indeed, the signal loss after 1 or 3 adjacent short microwave π pulses is approximately the same.

2.3 Decoherence sources

The quantronium is subject to decoherence due to its interactions with uncontrolled degrees of freedom inducing noise in $\lambda = N_g$ or $\lambda = \delta/2$ (we neglect here noise on E_J which has been shown to be non dominant). Decoherence is described here in terms of relaxation of the qubit energy into a quantum noise source on one hand, and in terms of random dephasing between the two qubit states due to adiabatic variations of ω_{01}, on the other hand. Each noise source is conveniently described by a quantum spectral density $S_\lambda(\omega) = 1/(2\pi)\int dt \langle \delta\lambda(0)\delta\lambda(t)\rangle \exp(-i\omega t)$ that quantifies, at positive ω, the ability of the source to absorb one energy quantum $\hbar\omega$. Classical spectral densities $Sc_\lambda(\omega) = 1/2\left[S_\lambda(-\omega) + S_\lambda(+\omega)\right]$ when $k_BT \gg \hbar|\omega|$ are also used. Figure 2 presents the main noise sources that have been identified, the actual circuit being represented as an effective equivalent circuit for decoherence.

The gate series impedance Z_g gives a spectral density [7-8]

$$S_{Ng}^G(\omega) = \kappa_g{}^2 \frac{\hbar^2\omega}{E_C^2}\left[1 + \coth\left(\frac{\hbar\omega}{2k_BT}\right)\right]\frac{\mathrm{Re}\left[Z_g(\omega)\right]}{R_k} \qquad (2.2)$$

with $\kappa_g = C_g/C_\Sigma$ and $R_k = h/e^2$. Using the parameters mentioned previously, we find

$$Sc_{N_g}^G(|\omega| < 2\pi.10\mathrm{MHz}) = (30\ \mathrm{ppb})^2/(\mathrm{Rad/s}) \qquad (2.3)$$

$$S_{Ng}^G(6\ \mathrm{GHz} < \omega < 17\ \mathrm{GHz}) = \left(1\text{-}3\ \mathrm{ppb}\right)^2/(\mathrm{Rad/s})\ . \qquad (2.4)$$

The admittance Y_R in parallel with the readout junction gives [7-8]

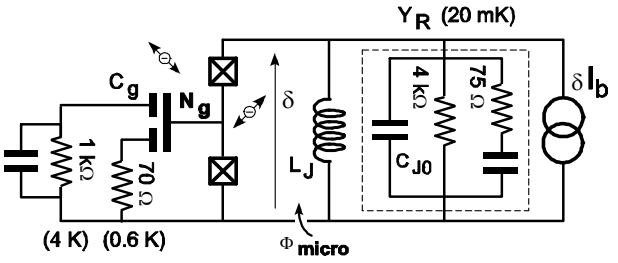

Figure 2. Equivalent circuit diagram for decoherence. The 70Ω and 1kΩ resistances represent the real part of the series gate impedance at the qubit frequency and at low frequency, respectively. Inductance L_J represents the readout junction whereas the 75Ω and 4kΩ resistances are parallel admittances at the qubit and at low frequency, respectively. Microscopic charged two-level fluctuators are displayed as double arrows and flux fluctuators are encapsulated in ϕ_{micro}.

$$S^R_{\delta/2\pi}(\omega) = \frac{\mathrm{Re}\left[Y_R(\omega)\right]}{\left(\varphi_0 \omega \left|Y_\delta\right|\right)^2} \frac{\hbar\omega}{2\pi}\left[1 + \coth\left(\frac{\hbar\omega}{2k_B T}\right)\right] \tag{2.5}$$

where Y_δ is the parallel combination of Y_R and of the readout junction inductance L_J. Using the actual parameters of the sample, we find

$$Sc^R_{\delta/2\pi}(|\omega| < 2\pi.10\mathrm{MHz}) = (30\ \mathrm{ppb})^2/(\mathrm{Rad/s}) \tag{2.6}$$

$$S^R_{\delta/2\pi}(6\ \mathrm{GHz} < \omega < 17\ \mathrm{GHz}) = \left(80\text{-}20\ \mathrm{ppb}\right)^2/(\mathrm{Rad/s})\ . \tag{2.7}$$

In addition, the noise δI_b of the pulse generator (AWG) has been measured to be white up to 200 MHz, and corresponds to a spectral density

$$Sc^{AWG}_{\delta/2\pi}(|\omega| < 2\pi.200\mathrm{MHz}) = (15\ \mathrm{ppb}/\cos\gamma)^2/(\mathrm{Rad/s}) \tag{2.8}$$

Besides, as any other Coulomb blockade device, the quantronium suffers from a Background Charge Noise (BCN) due to charged two-level fluctuators. The corresponding spectral density is of the *1/f* type at low frequency,

$$Sc^{BCN}_{N_g}(|\omega| < 2\pi.100\mathrm{kHz}) = A/|\omega|\,, \tag{2.9}$$

and has an amplitude A commonly found in the range $[10^{-6}, 10^{-7}]$ for the parameters of our experiment. Finally, as any other SQUID type device, the quantronium should experience a phase 1/f noise whose origin is unknown.

$$Sc^{micro}_{\delta/2\pi}(|\omega| < 2\pi.1\mathrm{kHz}) \sim A/|\omega| \qquad A \approx 10^{-10}\,. \tag{2.10}$$

2.4 Theoretical relaxation and decoherence rates

We consider here the case when, after its initial preparation, the effective spin precesses freely under the influence of the static field $\vec{H}$ set by the control parameters λ and of its classical and quantum fluctuations arising from the fluctuations $\delta\lambda$. One distinguishes two time scales, the relaxation time T_1 for the decay of the longitudinal Z component of the spin density matrix, and the decay time T_2 of the transverse part (coherence time). In addition, we also consider the case of spin-echoes, *i.e.* when a short pulse is

applied to the qubit in the middle of the period of free evolution in order to eliminate the effect of low frequency noise [5]. T_2 is in that case replaced by T_E.

Applying first the Fermi golden rule, one finds the relaxation rate [8]

$$T_1^{-1} = \pi D_{\lambda,\perp}^2 S_\lambda(\omega_{01})/2 \tag{2.11}$$

where $D_{\lambda,\perp}$ is the transversal component of $\vec{D}_\lambda = \hbar^{-1}\partial\vec{H}/\partial\lambda$. From the sample parameters we compute

$$D_{\delta/2\pi,\perp}\left(\delta = 0 \text{ or } N_g = 1/2\right) = 380\ d\left[1 + 6.0\left(\frac{\delta}{2\pi}\right)^2\right] \text{GRad/s} \tag{2.12}$$

$$D_{Ng,\perp}\left(\delta = 0 \text{ or } N_g = 1/2\right) = 193 \text{ GRad/s} \tag{2.13}$$

Then we compute [5,8] the average factors $f_{z,R}(t) = \left\langle \exp\left[i\varphi(t)\right]\right\rangle$ and $f_{z,E}(t) = \left\langle \exp\left[i\varphi_2(t/2) - i\varphi_1(t/2)\right]\right\rangle$ involving the phases $\varphi(t)$ or $\varphi_2(t/2) - \varphi_1(t/2)$ accumulated during a period t of free evolution with and without echo, respectively. Assuming that the noise δλ is Gaussian and assuming a non vanishing linear longitudinal coupling to the noise, $\partial\omega_{01}/\partial\lambda = D_{\lambda,z} \neq 0$, a simple semi-classical calculation gives [7-8]

$$f_{z,R}(t) = \exp\left[-\frac{t^2}{2} D_{\lambda,z}^2 \int_{-\infty}^{\infty} d\omega S_\lambda(\omega) \operatorname{sinc}^2\left(\frac{\omega t}{2}\right)\right] \tag{2.14}$$

$$f_{z,E}(t) = \exp\left[-\frac{t^2}{2} D_{\lambda,z}^2 \int_{-\infty}^{\infty} d\omega S_\lambda(\omega) \sin^2\left(\frac{\omega t}{4}\right) \operatorname{sinc}^2\left(\frac{\omega t}{4}\right)\right] \tag{2.15}$$

Taking now relaxation into account, the transverse polarization decays actually as $g(t) = f_z(t)\exp\left[-t/2T_1\right]$, T_2 and T_E being thus defined by $g(t) = \exp(-1)$. It is interesting to notice that when the noise power S_λ is smooth near $\omega \approx 0$, $f_{z,R}(t) = \exp\left(-t/T_\varphi\right)$ with $T_\varphi^{-1} = \pi D_{\lambda,z}^2 S_\lambda(0)$. From the sample parameters we compute

$$D_{\delta/2\pi,z}\left(\delta = 0 \text{ or } N_g = 1/2\right) = -850\ \frac{\delta}{2\pi} \text{ Grad/s} \tag{2.16}$$

$$D_{Ng,z}\left(\delta = 0 \text{ or } N_g = 1/2\right) = +290\ (N_g - 1/2) \text{ Grad/s}. \tag{2.17}$$

At P_0, the two $D_{\lambda,z}$'s vanish and a second order calculation of the dephasing involving $\partial^2\omega_{01}/\partial\lambda^2$ is required [10]. The sample parameters lead to $\partial^2\omega_{01}/\partial(\delta/2\pi)^2 = -850$ Grad/s and $\partial^2\omega_{01}/\partial(N_g)^2 = +290$ Grad/s.

3. EXPERIMENTAL CHARACTERIZATION OF DECOHERENCE DURING FREE EVOLUTION

3.1 Relaxation Time (T_1) measurement

Relaxation of the longitudinal polarization is measured form the decay of the switching probability p after a π pulse. Fits by an exponential decay [5] lead to the relaxation times T_1, which vary with P as shown in Fig. 3: T_1 is about 0.5 μs in the vicinity of P_0 and show rapid variations by a factor up to 4 away from P_0 in the phase direction. In the parameter range explored, the matrix element $D_{Ng,\perp}$ is approximately constant whereas $D_{\delta/2\pi,\perp}$ varies smoothly with δ by a factor of only 2. Consequently, the measured variation of T_1 reflects quite directly the variation with frequency of the density of environmental modes coupled to the qubit. Can the relaxation be fully attributed to the biasing and measuring circuit ? To answer this question, we compute at P_0, from Eq. (2.11) and from the noise spectra (2.4)-(2.7) due to

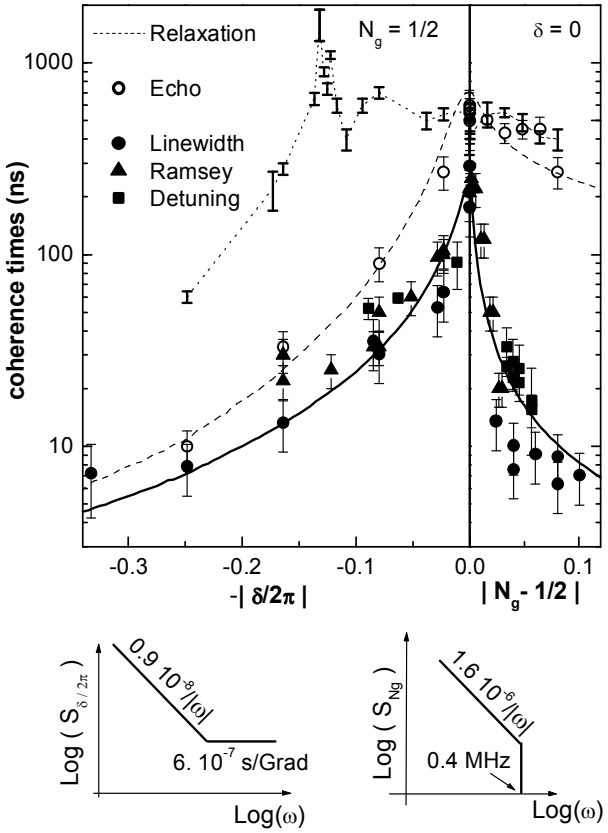

Figure 3. Summary of all the characteristic times, T_1 (dotted line), T_2 (solid symbols), and T_E (open circles), as a function of the biasing point. For T_2, the legend indicates the measurement method. The vertical line separating the two top frames corresponds to the optimal point P_0. The dashed and solid lines are fits of the T_2 and T_E's, assuming that N_g and δ noises have the modified 1/f spectral densities shown in the bottom. The fitting parameters are also indicated.

Z_g and Y_R, values of T_1 of about 2 μs and 3-6 μs, respectively. The combined effect of Z_g and Y_R gives thus $T_1 \approx 1-1.5\mu s$, which is 2-3 times longer that the measured value. We conclude that if our estimate of the circuit impedances is correct, a large part of the relaxation is also to be attributed to microscopic environmental modes. Nevertheless, estimating impedances above 14 GHz, as seen from the qubit, with a precision better than a factor 2 is in practise very difficult and relaxation could be due predominantly to the circuit.

3.2 Coherence time (T_2 and T_E) measurements

T_2 was determined by three different complementary methods. The first one is the Ramsey fringe method [2,5]. It consists in measuring directly the temporal decay of the average transverse polarization of the spin using two microwave π/2 pulses (detuned by a few tens of MHZ) just before and after the period Δt of free evolution. The switching probability at the end of the sequence oscillates with Δt at the frequency $\Delta\nu$, with amplitude that decays as $[1+g_R(\Delta t)]/2$, when neglecting small geometrical corrections due to detuning. The second method uses an adiabatic detuning N_g or δ pulse in the middle of a Ramsey sequence performed at the optimal point P_0 [5]. This detuning pulse moves the system temporarily during a time Δt_1 from P_0 to a point P where T_2 is to be measured. At constant Δt, the measured signal oscillates with Δt_1 at the new detuning frequency $\Delta\nu(P)$, with amplitude that decays with a characteristic time $T_2(P)$. The interest of the method is that the parameters of the Ramsey pulses can be optimized and kept constant for all points P. These first two methods are of course applicable only to points where $T_2 > 1/\Delta\nu(P)$. When T_2 is too short, it is more convenient to operate in the frequency domain, by recording the line shape of the resonance line at low microwave power (desaturated line). In this case the lineshape is the Fourier transform of the free precession signal. One has $T_2 = \alpha/(\pi\Delta\nu_{\mu w})$ where $\Delta\nu_{\mu w}$ is the full width of the line at its half maximum and α is a coefficient that depends on the exact shape of the line (1 for a lorentzian or 0.8 for a gaussian). Practically, desaturating the line leads to a rather low signal to noise ratio and it is difficult to discriminate between the two shapes. Now, near P_0, the Ramsey decays look close to exponential and we take $\alpha = 1$. Anyway, our error bars on T_2 are larger than the difference between the two α's. Spin-echo-like experiments were performed by inserting a microwave π pulse in the middle of a Ramsey sequence [8]. It was possible experimentally to vary the sequence duration Δt while keeping the π pulse precisely in the middle of the sequence. Using this protocol, one maps directly the echo maximal amplitude as a function of Δt [5]. In absence of detuning and decoherence, the two π /2 pulse and the π pulse induce a complete turn of

the spin so that the signal would be zero for any Δt. Dephasing makes actually the signal increase to its saturation value as $[1-g_E(\Delta t)]/2$. At finite $\Delta\nu$, a small oscillation of p adds on top of this increase. This oscillation has an amplitude that decays essentially as $g_R(\Delta t)$. By fitting exactly a few echo curves, we have checked that the effect of these small oscillations and also of experimental errors on the pulse durations have no big effect on the determination of T_E values.

Examples of the experimental signals recorded with the all the methods described above have already been published [2,5]. Exhaustive results will also be published in a longer article. We summarise here all T_1, T_2 and T_E values obtained at different P on Fig. 3, which is the main result of this paper.

3.3 Discussion

Figure 3 shows first that decoherence of this quantronium is limited at all P by pure dephasing rather than by relaxation. Nevertheless $T_E(P_0)$ approaches the limit $2T_1$. Then, it shows that Ramsey decays, "detuning pulses", and lineshapes measurements lead to T_2's in reasonable agreement. It also validates clearly the concept of optimal point P_0, where T_2's and T_E's are maximum. The echoes happen to be much more efficient at and away from P_0 in the charge direction, where $T_E/T_2 \in [2-40]$, than away from P_0 in the phase direction. This clearly shows that a large part of the charge noise is at frequency lower than $1/T_E \approx 1\text{MHz}$. Another important result is that the T_2's are far too short for the decoherence to be explained by the dissipative elements of the circuit. Indeed, injecting the spectral densities (2.3), (2.6) and (2.8) in Eqs. (2.14)-(2.17) lead to theoretical $T_2(P_0)$ values of a fraction of a tenth of second for the gate line, of 160µs for the readout impedance and of 7 µs for the pulse generator white noise, respectively. The main sources of noise are thus of microscopic nature. Their spectral densities being known to be essentially of the 1/f type, we have tried to fit the data with pure 1/f spectra, using Eqs. (2.14)-(2.17). Whereas fits were good for the T_2's, we computed $T_E/T_2 \approx 4$ everywhere, as expected from [8], which is very different from the data. Consequently, we introduce purely empirically a high frequency cut-off in the charge noise and add a white contribution to the phase noise as shown in Fig. 3. The corresponding best fits (also on the figure) are now in better agreement with the data. Note that the second order contribution of the noises at and very close to P_0 was roughly estimated assuming gaussian N_g^2 or δ_g^2 noises. Nevertheless, more accurate estimations lay in our experimental error bars and confirm that the main contribution to decoherence at P_0 is from microscopic charge noise. The fitted amplitude $A = 1.6\ 10^{-6}$ of the 1/f charge noise is in the expected range whereas that for the phase noise, $A = 0.9\ 10^{-8}$,

is 100 times larger than expected from literature. The cut-off fitted at 0.4 MHz was not expected and would be interesting to check with a fast electrometer experiment. Finally, the amplitude 6 10^{-16}/(Rad/s) of the white phase noise happens to be very close to that expected from the readout pulse generator.

4. CONCLUSION

We have characterized decoherence in the quantronium using techniques adapted from NMR and atomic physics. We have found that whereas relaxation might be limited by the circuit, microscopic noise sources are responsible for decoherence. We have validated the concept of optimal point P_0 and shown that for $E_J/E_C \sim 1$, the main source of decoherence at P_0 is charge noise. We have analysed the data using a simple model for the interaction of the qubit with its environment and for the noise. A more complete analysis including decoherence during driven evolution will be published later.

Acknowledgements: The essential technical contribution of P.F. Orfila, P. Senat and J.C. Tack, and the financial support from the european SQUBIT2 contract are gratefully acknowledged.

References

[1] Y. Nakamura, Yu. A. Pashkin, J. S. Tsai, Nature **398**, 786 (1999).
[2] D. Vion *et al.*, Science **296**, 886 (2002).
[3] I. Chiorescu et al., Science 299, 1869 (2003).
[4] M. A. Nielsen and I. L. Chuang, *Quantum Computation and Quantum Information* (Cambridge University Press, Cambridge, 2000).
[5] E. Collin *et al.*, Phys. Rev. Lett. 93, 157005 (2004).
[6] V. Bouchiat *et al.*, Phys. Scr. T76, 165 (1998).
[7] A. Cottet, PhD thesis, Université Paris VI, (2002); *www-drecam.cea.fr/drecam/spec/Pres/Quantro/*
[8] D. Vion, in *Quantum entanglement and information processing*, D. Estève, J.M. Raimond, and J. Dalibard eds, (Elsevier, 2004).
[9] G. Ithier *et al.*, under press by Phys. Rev. Lett.
[10] Y. Makhlin and A. Shnirman, Phys. Rev. Lett., 92, 178301 (2004).
[11] E. Paladino *et al.*, cond-mat/0407484 (2004).